Solar panels as air Cherenkov detectors for extremely high energy cosmic rays

S. Cecchini [a,d], I. D'Antone [a], L. Degli Esposti [a], G. Giacomelli [a], M. Guerra [b], I. Lax [a], G. Mandrioli [a], A. Parretta [c], A. Sarno [c], R. Schioppo [b], M. Sorel [a*], M. Spurio [a]

[a] Dipartimento di Fisica dell'Università di Bologna and INFN Sezione di Bologna, 40126 Bologna, Italy
[b] ENEA, Area Sperimentale di Monte Aquilone, 71043 Manfredonia (FG), Italy
[c] ENEA, Centro Ricerche, 80055 Portici (NA), Italy
[d] Istituto TESRE/CNR, 40129 Bologna, Italy

arXiv:hep-ex/0002023v1 7 Feb 2000

Increasing interest towards the observation of the highest energy cosmic rays has motivated the development of new detection techniques. The properties of the Cherenkov photon pulse emitted in the atmosphere by these very rare particles indicate low-cost semiconductor detectors as good candidates for their optical read-out.

The aim of this paper is to evaluate the viability of solar panels for this purpose. The experimental framework resulting from measurements performed with suitably-designed solar cells and large conventional photovoltaic areas is presented. A discussion on the obtained and achievable sensitivities follows.

1. INTRODUCTION

The flux of Extremely High Energy Cosmic Rays (EHE CRs) is very low: $\phi(E > 10^{19}\ eV) \simeq 0.5\ km^{-2}yr^{-1}sr^{-1}$, and few hundreds of events have been recorded with energies above $10^{19}\ eV$ [1]. Past and present experiments generally agree on the slope of the energy spectrum and on its absolute intensity below $E \simeq 4 \cdot 10^{19}\ eV$; however, no firm conclusion can be drawn on the existence of events above the Greisen-Zatsepin-Kuz'min cut off in CR energy [2], on anisotropy of the arrival directions and correlation with cosmic point sources [3], and on CR composition [4].

EHE cosmic rays are indirectly detected using several techniques: either through ground array experiments, which measure the lateral distribution of electrons and muons in the extensive air shower (EAS) using scintillation counters or water Cherenkov tanks; or through experiments sensitive to the UV photons emitted by nitrogen fluorescence generated in the atmosphere at the passage of the shower particles.

Cherenkov light is also produced in the atmosphere by the electrically charged particles in the shower; this flux ρ_C has a broad spatial distribution at sea level, with a lateral extent reaching several km away from the EAS core for very energetic and inclined showers. Since ρ_C roughly scales with CR energy, this light can be very intense: $\rho_C \simeq 10^{10}$ photons/m^2 for $10^{19}\ eV$ vertical CRs near the shower core [5], as shown in Fig.1.

The Cherenkov photons reach sea level as a plane wave, in a front with a typical duration of tens of ns near the shower axis, and few μs at several km from the core. The spectral distribution of the Cherenkov light at sea level ranges between 300 nm and 1500 nm.

The properties of the Cherenkov pulse suggest the possibility to observe in a different way the highest energy CRs by means of low-cost semiconductor photodetectors, including solar panels [6]. Solar panels are composed of electrically connected solar cells, i.e. n-p junctions with a large surface area. Solar cells have a high quantum efficiency (QE), with a broad maximum between 600 nm and 1000 nm, well matching the Cherenkov spectral distribution at sea level ($\langle QE \rangle_{\check{C}} \simeq 0.55 \div 0.60$). The aim of this work is to experimentally investigate the viability of EHE cosmic rays observation using solar panels as air Cherenkov detectors.

*Corresponding author: SOREL@BO.INFN.IT

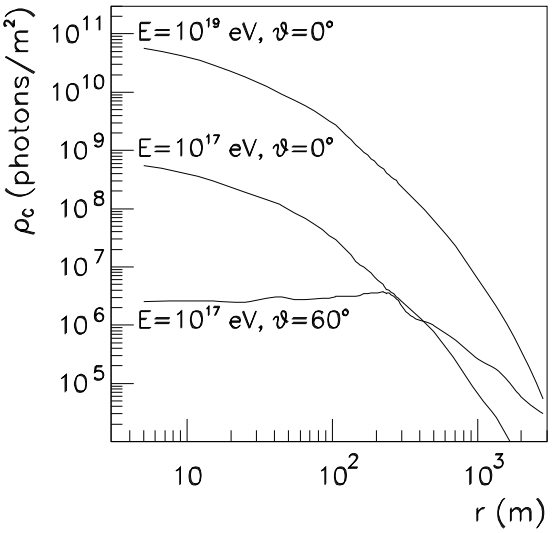

Figure 1. Cherenkov flux ρ_C (photons/m^2) versus distance r from the shower core for different CR energies and zenith angles.

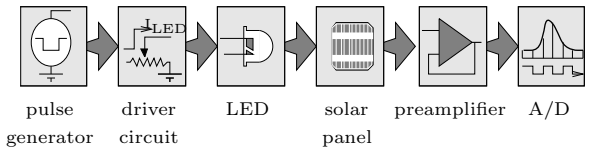

Figure 2. Block diagram of the experimental setup used to evaluate the response of solar cells/panels to light pulses.

2. EXPERIMENTAL SETUP

One of the main concerns is the evaluation of the response of single solar cells and panels to faint light pulses. Fig.2 shows a schematic diagram of the experimental setup used for this purpose.

In order to simulate the Cherenkov pulses, we used LEDs with fast response ($\simeq 15\ ns$) and good pulse-to-pulse reproducibility. Light flashes are produced through a driver circuit which allows both pulse duration and pulse intensity control. Suitable optical pulses were obtained, with $10^7 \div 10^{10}$ photons emitted per pulse, spread over a time duration of $100\ ns < \Delta t < 1\ \mu s$.

The photoelectric transient pulse produced by the cell/panel is decoupled from the continuous component through a capacitor or a pulse transformer and fed into a preamplifier; the resulting signal is then digitized and recorded.

Particular attention has been devoted to the evaluation of the luminous power emitted by the LEDs; for this purpose we used different methodologies, both direct power measurements through large area calibrated sensors and measurements based on integrating spheres which are independent from light beam geometry. We have tested monocrystalline, polycrystalline and amorphous Silicon solar cells with different active areas (from 4 cm^2 to 100 cm^2), and their grouping in panels and rows of panels through series or parallel connections. Tests included both commercial products and custom designed detectors in order to improve their transient response.

The choice of the preamplifier to be used with solar cells/panels is a difficult task, and reflects the unusual properties of these photodetectors; both charge and voltage preamplifiers were tested. Charge preamplifiers are usually preferred with semiconductor detectors for their more stable voltage-to-charge gain, insensitive to the properties of the detector. However, they are typically designed for capacitive detectors in the pF to nF range, a condition which does not apply to solar cells/panels. The net effect is that charge preamplifiers behave in a "non ideal" way. The ORTEC 142B charge preamplifier has shown to be a good candidate; a typical solar cell pulse obtained with this amplifier is shown in Fig.3.

3. SIGNAL CONSIDERATIONS

In general, the speed of response of a photodiode is limited by the combination of three factors: carrier diffusion to the junction; drift time through the depletion region; effect of the charge storage in the depletion region, which can be expressed through the junction capacitance C_d. In the case of a solar cell, the main limitation is given by C_d, which is very high due to the low p-substrate resistivity and the large surface area. The cell may then be modelled as a photocurrent

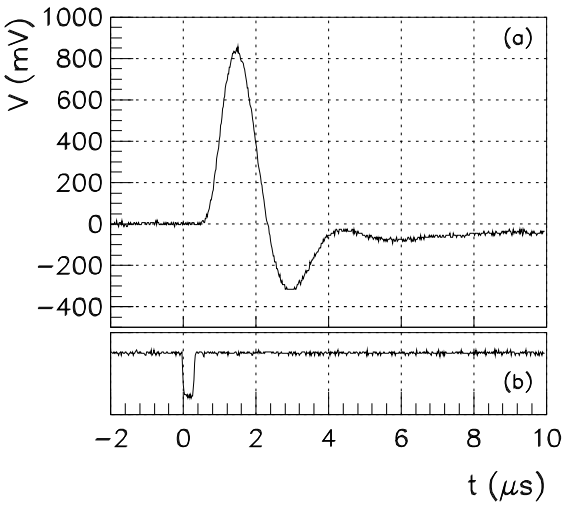

Figure 3. (a) Typical solar cell response with an ORTEC 142B preamplifier to a $\Delta t = 300\ ns$ light flash; (b) square pulse driving the LED emission.

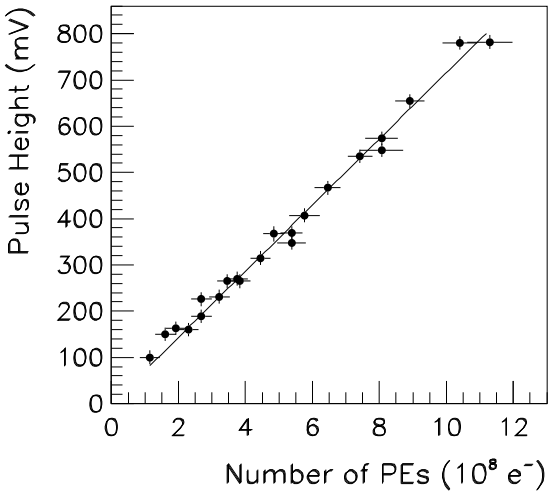

Figure 4. Pulse height versus number of photoelectrons for a 78 cm^2 solar cell. The amplifier used is the ORTEC 142B.

source in parallel to the junction capacitance; a cell shunt resistance R_d has also to be considered to take into account the high leakage currents [7].

We have verified that solar cells/panels behave as capacitive detectors by means of the pulse shape analysis of the photoelectric voltage observed through different load resistances; pulse shapes typical of a resistive charging of a capacitance were obtained.

3.1. Voltage-to-charge linearity and gain

Fig.4 shows the linear relationship between the pulse height of the solar cell signal and the total photogenerated charge in the pulse, expressed as the number of photoelectrons (PEs). Signals in Fig.4 were obtained with different LEDs, varying intensities and pulse durations ($100\ ns < \Delta t < 1\ \mu s$). From the slope of the linear fit we evaluated the voltage-to-charge gain.

The measured voltage-to-charge ratio is dependent from C_d; moreover, it is lower by a factor of $10^2 \div 10^3$ than what predicted by an ideal charge preamplifier, especially for the higher capacitance detectors tested (see Tab.1).

Since the quantum efficiency is very similar for different cells, the detector capacitance is the main factor of merit for signal amplitude considerations, and must be reduced as much as possible. The use of higher resistivity substrates (even very large area PIN diodes) is a possible solution to further lower C_d, thereby increasing the preamp gain.

Table 1
Cell area, cell capacitance C_d and measured gain for two cells of different areas and made from the same bulk material. The specified gain of the amplifier is $500 \cdot 10^{-3}\ V/pC$.

Area (cm^2)	C_d (μF)	Gain ($10^{-3}\ V/pC$)
9	0.6 ± 0.1	3.5 ± 0.3
96	6.1 ± 1.4	0.7 ± 0.2

3.2. Solar cells grouping into modules

An advantage of solar cells over other photodetectors is that they can easily be connected to give 1 m^2 or more active area, thus collecting more Cherenkov light. As shown in Fig.5, we observed that a series connection of identical solar cells does not decrease the gain; then, increasing the number of series connected cells gives rise to a proportionally higher Cherenkov signal.

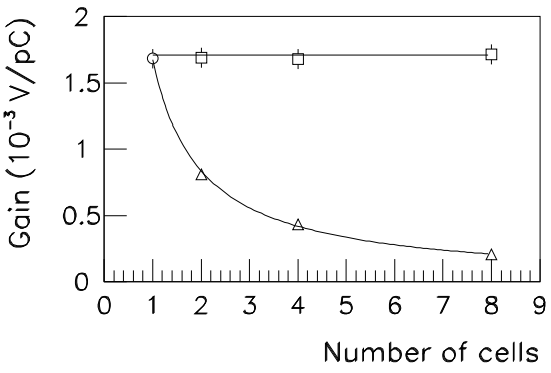

Figure 5. Voltage-to-charge gain for different electrical connections of identical cells. □: series connection; △: parallel connection.

3.3. Effect of background light

An important aspect concerning the duty cycle of solar panels as CR detectors is the gain degradation due to background light; in particular, the photovoltaic forward voltage due to ambient light increases the capacitance of the cells even further. Low impedance transformers allow to short out the DC photovoltaic voltage, and no significant signal degradation is observed even during daytime. This is not the case for solar panels working in open-circuit conditions, where the AC variation is obtained through a capacitive DC decoupler: gain degradation is observed even in dusk/dawn conditions (Fig.6). However, in both cases the solar panel sensitivity may decrease during daytime due to additional shot-noise.

4. DETECTOR NOISE AND SENSITIVITY

For noise evaluation purposes, the solar cell equivalent circuit described above [7] must be extended to include also series and parallel noise generators, which are dependent not only from the detector alone, but also from the preamplifier and shaper characteristics. In particular, the Equivalent Noise Charge (ENC) is lower for low junction capacitance, high shunt resistance cells, low series noise preamplifiers and long shaping times [8]. Moreover, if the cell operates in the photovoltaic mode (no reverse bias applied) and under limited background light, the shot-noise contribution to ENC may be neglected. For our $10 \times 10\ cm^2$ mono-Si cell and amplifier, we evaluated $\mathrm{ENC_{rms}} \simeq 8 \cdot 10^6\ e^-$, in good agreement with the observed value.

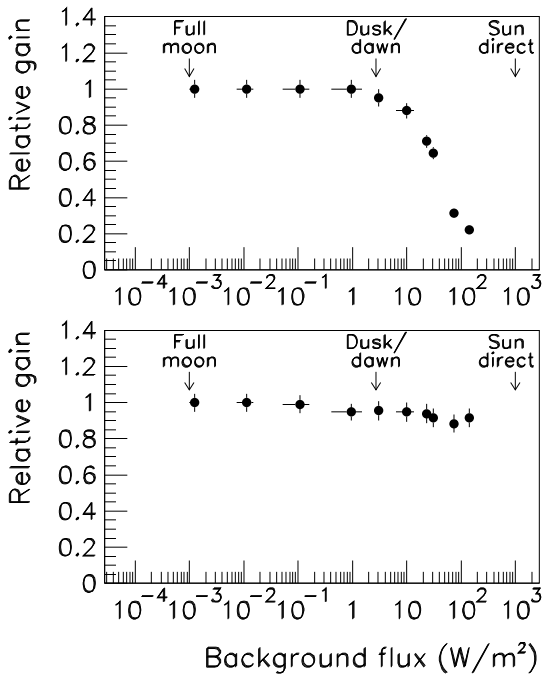

Figure 6. Pulse height degradation due to background light. Top: DC decoupling through capacitance; bottom: DC decoupling through low impedance pulse transformer.

Adding more series connected cells, RF pickup from the electrical connections in the panel becomes progressively the main source of noise. The fact that RF noise increases with detector area was clearly verified from observations performed on the 30 m^2 rows of an experimental photovoltaic plant operated by ENEA at Manfredonia (Italy). As single panels are used, proper RF shielding is obtained using Faraday cages; in this way, we do not observe any significant variation in ENC in increasing the number of series connected cells.

Fig.7 shows the signal-to-noise ratio in dark

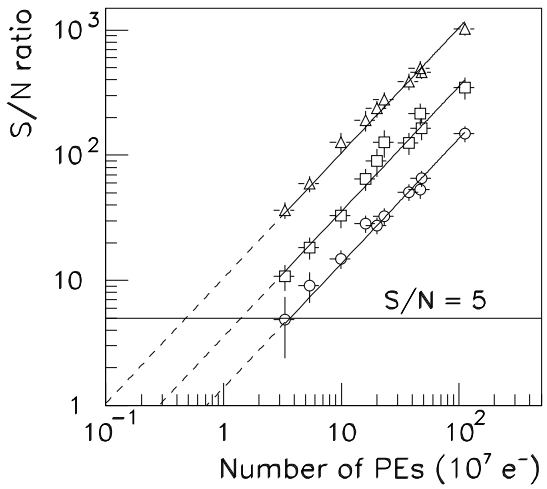

Figure 7. Signal-to-noise ratio versus the number of PEs for three different solar panels. ◯: $36 \cdot 96\ cm^2$ mono-Si cells; □: $32 \cdot 32\ cm^2$ a-Si cells; △: $36 \cdot 9\ cm^2$ mono-Si cells.

conditions plotted versus the number of PEs, for three different panels. These are a mono-Si 0.35 m^2 module (Italsolar 36 MS-CE), an a-Si 0.10 m^2 module (Solarex SA-5), and a special mono-Si 0.032 m^2 module manufactured from EUROSOLARE to test smaller area cells. Considering a trigger threshold of 5σ, the PE sensitivity per unit area is $\simeq 10^8\ e^-/m^2$, similar for the three panels and comparable to the charge per unit area produced in the panels by the Cherenkov flux of $10^{17}\ eV$ vertical CRs near the shower core (see Fig.1).

5. SIMULATION OF CR DETECTION CAPABILITIES

To give a quantitative idea of CR detection capabilities of solar panel detectors, we have considered both a small array for $\sim 10^{17} \div 10^{18}\ eV$ CRs, and a larger one for the highest energy CRs. Their characteristics are given in Tab.2.

The predictions are based on Cherenkov lateral and spectral distributions from a modified MOCCA code including Cherenkov light production and attenuation in atmosphere [5]. CRs are generated as primary protons with isotropic arrival directions and with energies according to the observed CR flux [9]. Knowing the Cherenkov flux reaching the detectors, the panels quantum efficiency weighted on the Cherenkov spectrum and the effective area of the detector seen by the Cherenkov wave plane, one can deduce the photogenerated charge in the detectors.

Table 2
Two possible arrays for CR detection.

	A	B
Number of det.	16	256
Det. spacing	50 m	500 m
Array config.	rectangular grid	
Det. type	mono-Si panel (36 series cells)	
Det. area	0.35 m^2	
Det. orientation	flat, horizontal	
Det. sensitivity	$3.6 \cdot 10^7\ e^-$	

5.1. Event rate and energy spectrum

Fig.8 shows the event rate and the event energy distribution for the two arrays of Tab.2, for different thresholds on the number of triggered detectors. Both arrays give $\simeq 1$ event/day when three triggered detectors are required. This rate may decrease by a factor of $2 \div 3$ when meteorological conditions and background light are taken into account.

5.2. Sky coverage

We also evaluated the solid angle of acceptance for the array B of Tab.2. This array should give almost uniform sky coverage up to $\simeq 60^o$. For greater zenith angles very few CRs are observable with horizontal detectors, because of the lower Cherenkov flux, the smaller detector effective area and the higher reflectivity of the panels coating. It has been proposed to use several panels oriented towards different regions of the sky for each detector, in order to reconstruct the CR arrival direction even with no timing information [10]. In this way a complete sky coverage could also be obtained.

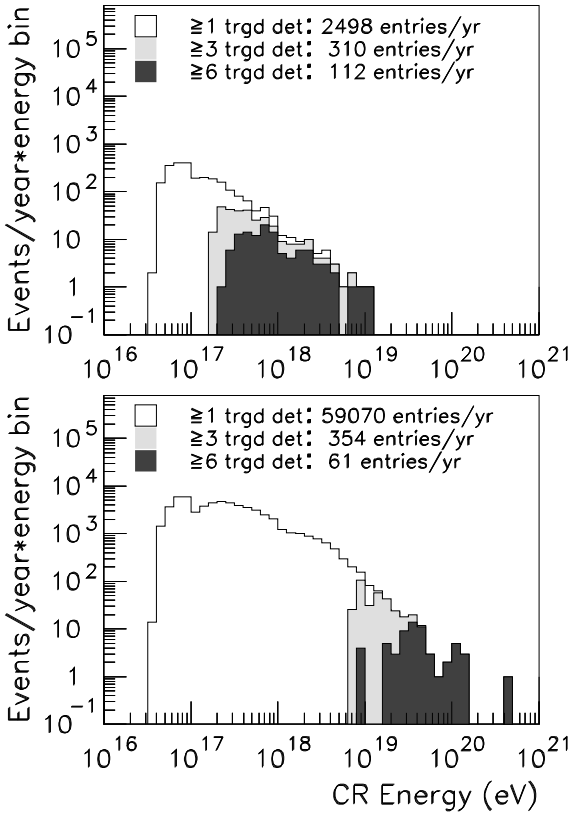

Figure 8. Energy spectrum of detectable CRs with the array A (top) and the array B (bottom). The statistics refers to one year of simulated data-taking. The total number of events for different trigger conditions is also given.

6. CONCLUSIONS

The response of solar panels to light pulses was investigated both theoretically and experimentally. These devices show excellent quantum efficiency and linearity; satisfactory sensitivities have been reached ($\simeq 10^8\ e^-/m^2$). Optimization of solar panels for Cherenkov light detection is possible, but even commercial modules seem to be adequate.

A Monte-Carlo study was performed in order to predict CR detection capabilities of possible arrays. The results indicate that the technique may be tested at $\sim 10^{17}\ eV$ energies, allowing an evaluation of the accuracy in the reconstruction of shower parameters. In conclusion, cost-effective solar panels could be strong candidates for the detection of the EHE CRs.

ACKNOWLEDGEMENTS

The authors would like to express their gratitude to D. B. Kieda for the original idea on this detection technique and for several data used in the Monte-Carlo calculations. We acknowledge M. Bruno, G. Martinelli and G. Tomassetti for their suggestions and their kind supply of electronics instrumentation. We are also indebted to R. Peruzzi from EUROSOLARE (Nettuno, Italy) for providing us with solar panels specifically manufactured for this work.

REFERENCES

1. J. Linsley, *Phys. Rev. Lett.* **10** (1963) 146; S. Yoshida et al., *Astropart. Phys.* **3** (1995) 105; A. A. Watson, *Nucl. Phys. (Proc. Suppl.)* **22B** (1991) 116.
2. K. Greisen, *Phys. Rev. Lett.* **16** (1966) 748; G. T.Zatsepin and V. A. Kuz'min, *JETP Lett.* **4** (1966) 78.
3. T. Stanev et al., *Phys. Rev. Lett.* **75** (1995) 3056; E. Waxman, K. B. Fischer and T. Piran, preprint astro-ph/9604005; N. Hayashida et al., *Phys. Rev. Lett.* **77** (1996) 1000; D. J. Bird et al., *Astrophys. J.* **441** (1995) 144.
4. K. Bernlöhr et al., *Proc. 25th ICRC* **4** (1997) 65; D. J. Bird et al., *Proc. 23rd ICRC* **2** (1993) 38.
5. D. B. Kieda, private communication.
6. D. B. Kieda, *Astropart. Phys.* **4** (1995) 133.
7. S. M. Sze, *Physics of semiconductor devices*, 2nd Ed., John Wiley & Sons (1981).
8. E. Gatti and P. F. Manfredi, *Nuovo Cimento* **9** (1986) 53.
9. A. A. Watson, *Proc. 19th ICRC* **9** (1985) 111.
10. D. J. Suson and D. B. Kieda, *Nucl. Instr. Meth.* **A374** (1996) 381.